



Since January 2020 Elsevier has created a COVID-19 resource centre with free information in English and Mandarin on the novel coronavirus COVID-19. The COVID-19 resource centre is hosted on Elsevier Connect, the company's public news and information website.

Elsevier hereby grants permission to make all its COVID-19-related research that is available on the COVID-19 resource centre - including this research content - immediately available in PubMed Central and other publicly funded repositories, such as the WHO COVID database with rights for unrestricted research re-use and analyses in any form or by any means with acknowledgement of the original source. These permissions are granted for free by Elsevier for as long as the COVID-19 resource centre remains active.



Instrument-free, CRISPR-based diagnostics of SARS-CoV-2 using self-contained microfluidic system

Ziyue Li^{a,b}, Xiong Ding^a, Kun Yin^a, Lori Avery^c, Enrique Ballesteros^c, Changchun Liu^{a,*}

^a Department of Biomedical Engineering, University of Connecticut Health Center, 263 Farmington Ave., Farmington, CT, 06030, United States

^b Department of Biomedical Engineering, University of Connecticut, 260 Glenbrook Road, Storrs, CT, 06029, United States

^c Department of Pathology and Laboratory Medicine, University of Connecticut Health Center, Farmington, CT, 06030, United States

ARTICLE INFO

Keywords:

SARS-CoV-2 detection
CRISPR-Cas12a
Instrument-free molecular diagnostics
Self-contained microfluidic chip
Hand warmer

ABSTRACT

Rapid and sensitive detection of severe acute respiratory syndrome coronavirus 2 (SARS-CoV-2) is critical for early diagnostics and timely medical treatment of coronavirus disease 2019 (COVID-19). However, current detection methods typically rely on expensive and bulky instrumentation. Here, we developed a simple, sensitive, instrument-free, CRISPR-based diagnostics of SARS-CoV-2 using a self-contained microfluidic system. The microfluidic chip integrates isothermal amplification, CRISPR cleavage, and lateral flow detection in a single, closed microfluidic platform, enabling contamination-free, visual detection. To simplify the operation and transportation of the device, we lyophilized the CRISPR reagents in the reaction chamber and pre-stored the liquid solutions in blisters. We employed a low-cost, portable hand warmer to incubate the microfluidic chip without the need for electricity. The self-contained microfluidic system can detect down to 100 copies of SARS-CoV-2 RNA. Further, we clinically validated our method by detecting 24 COVID-19 clinical nasopharyngeal swab samples, achieving excellent sensitivity (94.1%), specificity (100%), and accuracy (95.8%). This simple, sensitive, and affordable microfluidic system represents a promising tool for point-of-care diagnostics of COVID-19 and other infectious diseases.

1. Introduction

The coronavirus disease 2019 (COVID-19) pandemic caused by severe acute respiratory syndrome coronavirus 2 (SARS-CoV-2) has spread all over the world and severely threatens human health. As of now, the pandemic has resulted in more than 240 million confirmed cases and more than 4.9 million deaths worldwide, according to the World Health Organization ([WHO Coronavirus \(COVID-19\) Dashboard](https://www.who.int/dashboards/coronavirus)). Rapid, sensitive, and early molecular diagnostics of COVID-19 is crucial for preventing transmission and providing patients with timely care ([Patchsung et al., 2020](#)). Quantitative real-time polymerase chain reaction (PCR) with reverse transcription (RT-qPCR), which measures the quantity of viral RNA, remains the gold-standard technique for SARS-CoV-2 detection ([Vogels et al., 2020](#)) due to its high sensitivity and specificity. However, current RT-qPCR assays typically require expensive instruments, well-trained personnel, and dedicated laboratory space, all of which reduce its utility in resource-limited settings.

In recent years, clustered regularly interspaced short palindromic repeats (CRISPR)-associated (Cas) proteins (e.g., Cas12a and Cas13a)

have emerged as powerful tools for nucleic acid-based molecular detection. In particular, researchers have combined isothermal amplifications, such as recombinase polymerase amplification (RPA), loop-mediated isothermal amplification (LAMP), rolling circle amplification (RCA), with CRISPR detection to develop highly sensitive and specific CRISPR-based molecular diagnostics technologies ([Ali et al., 2020](#); [Tian et al., 2020](#); [Wang et al., 2021](#); [Li et al., 2021](#)). Among them, RPA is one of the most popular amplification techniques for CRISPR-based molecular detection due to its simplicity, rapidity, high sensitivity and low reaction temperature. However, most of RPA/CRISPR assay methods involve multiple manual operations to transfer amplification products in an open system, which potentially increases the carry-over contamination risk. In addition, they require cold chain (e.g., freezer) for reagent delivery and storage, and complex electric equipment for heating and detection, both of which are not ideal for point-of-care diagnostic applications.

The integration of CRISPR-based molecular detection into microfluidics technology provides a new paradigm in next-generation medical diagnostics, especially point-of-care diagnostics. For instance, advances

* Corresponding author.

E-mail address: chaliu@uchc.edu (C. Liu).

<https://doi.org/10.1016/j.bios.2021.113865>

Received 28 October 2021; Received in revised form 2 December 2021; Accepted 3 December 2021

Available online 8 December 2021

0956-5663/© 2021 Elsevier B.V. All rights reserved.

have led to an electric field-driven microfluidic chip for rapid CRISPR-based diagnostics of SARS-CoV-2 in raw nasopharyngeal swab samples (Ramachandran et al., 2020) as well as an amplification-free microfluidic chip-based method for SARS-CoV-2 detection via mobile phone microscopy (Fozouni et al., 2021). However, these microfluidic diagnostic platforms still rely on relatively bulky electronic instrument and complex fluorescence detection system. Therefore, there is an unmet need for a rapid, easy-to-use, and affordable microfluidic diagnostic system for SARS-CoV-2 detection without the requirement for expensive equipment or well-trained personnel.

In this study, we have developed an instrument-free, hand warmer-powered, self-contained microfluidic system for SARS-CoV-2 detection in clinical samples. The microfluidic chip integrates reverse transcription RPA (RT-RPA) amplification, CRISPR-Cas12a cleavage reactions, and lateral flow (LF) detection in a single, closed microfluidic platform, enabling self-contained, contamination-free visual detection. To facilitate operation and transport, we lyophilized the CRISPR reagents in the CRISPR reaction chamber and pre-stored the liquid solutions in blisters. In addition, we employed a low-cost hand warmer pouch as a heating source to power the microfluidic chip, eliminating the need for a complex electric heater. To demonstrate clinical utility, we used the self-contained microfluidic system to detect COVID-19 clinical samples and demonstrated high sensitivity and specificity. Our simple, affordable, and sensitive molecular diagnostic platform represents a promising tool for point-of-care diagnostics of COVID-19 and other infectious diseases in resource-limited settings.

2. Experimental section

2.1. Reagents, materials, and apparatus

All oligonucleotides, CRISPR RNA (crRNA), and reporters (Supporting Information Table S1) were synthesized or purchased from Integrated DNA Technologies (IA, USA). SARS-CoV-2 RNA positive controls (GenBank: MN908947.3, Part#102024) were purchased from Twist Bioscience (CA, USA). LbCas12a, 10× NEBuffer 2.1, AMV Reverse Transcriptase, RNase H, and nuclease-free (NF) water were purchased from New England Biolabs (MA, USA). The Twist Amp Liquid Basic Kit and Milenia HybriDetect 1 were obtained from Twist Dx Limited (Maidenhead, UK). The QIAamp Viral RNA Mini Kit was purchased from Qiagen (MD, USA). The GoTaq® Probe 1-Step RT-qPCR System was purchased from Promega (WI, USA). All other chemicals used were of analytical reagent grade from Sigma Aldrich (MO, USA).

Blisters were purchased from Microfluidic Chip Shop (Jena, Germany). Microseal 'B' PCR Plate Sealing Film was obtained from Bio-Rad (CA, USA). Hand warmers were obtained from Kobayashi Healthcare International (GA, USA). Form 2 3D printer was purchased from FormLabs (MA, USA) and FreeZone 2.5-L benchtop freeze dry system from Labconco Corporation (MO, USA). Fluorescence signals were monitored in real time using the Bio-Rad CFX96 Touch Real-Time PCR Detection System (Bio-Rad Laboratories, CA). Endpoint fluorescence visual detection of the reaction tubes was accomplished with either the ChemiDoc MP Imaging System (Bio-Rad Laboratories, CA) or an LED blue light illuminator (Maestro UltraSlim).

2.2. Self-contained microfluidic system fabrication

Microfluidic chips and hand warmer-powered heater cases were first designed using Solidworks (Supporting Information Fig. S1) and fabricated by a Form 2 3D printer using clear resin. Next, the 3D-printed devices were washed with isopropyl alcohol for at least 30 min and cured in the hood for 24 h. To pre-store the reagents in the CRISPR reaction chamber, the CRISPR reaction reagents (LbCas12a, crRNA, and 1X NEBuffer 2.1) were lyophilized in the CRISPR reaction chamber by using a benchtop freeze dry system (auto set or -40°C and 0.1 mbar). Then, two blisters were fixed on the microfluidic chip using double-

sided tape. For 100 μL blister, nuclease-free water was pre-filled. For 200 μL blister, the dilution buffer (Milenia HybriDetect 1 kit) was pre-filled. Cotton was applied to separate chambers. Then, a lateral flow dipstick (Milenia HybriDetect 1 kit) was inserted into the lateral flow chamber of the chip. Lastly, the chip was sealed using Bio-Rad sealing films.

2.3. RT-RPA/CRISPR reaction system

The final RT-RPA reaction system contained 1X reaction buffer, 1X basic E-mix, 1X core reaction buffer, 0.1 U/ μL RNase H, 0.4 U/ μL AMV, 14 mM MgOAc, 0.5 μM each for forward and reverse primers, 0.8 mM for each nucleotide (dATP, dTTP, dCTP, dGTP), and 1 μL sample. The final volume of the CRISPR reaction was 30 μL containing 400 nM LbCas12a, 400 nM crRNA, 1X NEBuffer 2.1 (50 mM NaCl, 10 mM Tris-HCl, 10 mM MgCl₂, 100 $\mu\text{g}/\text{mL}$ BSA, pH 7.9, 25 $^{\circ}\text{C}$), RPA product, and reporter. For fluorescence detection in the reaction tubes, 5 μM fluorescein molecule (FAM)-ssDNA-quencher (ssDNA-FQ) was used. For lateral flow detection in the microfluidic system, 0.5 μM Biotin-ssDNA-FAM probe (ssDNA-BF) was used.

2.4. Microfluidic system operation and instrument-free readout

The microfluidic system includes a self-contained microfluidic chip and hand warmer-powered heater case. First, the RT-RPA reaction mixture was introduced into the RPA reaction chamber of microfluidic chip. Then, the chip was inserted into the heater case that was powered by a hand warmer pouch. After a 15 min-incubation, the RPA amplicons in the RPA reaction chamber was moved to the CRISPR reaction chamber by gently pressing the water blister with a finger, which rehydrated the lyophilized CRISPR reagent in the chamber. After a 45 min-incubation, the dilution buffer in the buffer blister was discharged by finger pressure and mixed with the CRISPR reaction products in the collection chamber. Then, the chip was placed vertically to allow the diluted CRISPR reaction products to contact the lateral flow dipstick. Lastly, the visual test results could be directly observed with the naked eye from the lateral flow dipstick in the detection chamber.

2.5. SARS-CoV-2 clinical sample preparation and RT-qPCR detection

Twenty-four de-identified clinical nasopharyngeal swab samples were used to test our self-contained microfluidic system under the approval of the Institutional Review Board of the University of Connecticut Health Center (protocol #P61067). The SARS-CoV-2 viral RNA samples were extracted from clinical samples using the QIAamp Viral RNA Mini Kit according to the manufacturer's protocol. A real-time fluorescence RT-qPCR assay was used to detect SARS-CoV-2 RNA according to the U.S. Centers for Disease Control and Prevention (CDC) 2019-Novel Coronavirus (2019-nCoV) Real-Time RT-qPCR Diagnostic Panel (CDC, 2020). The GoTaq Probe 1-Step RT-qPCR kit recommended by the CDC was used to prepare the RT-qPCR reaction solution. The 15 μL RT-qPCR mix included 1 \times GoTaq Probe Master Mix, 0.5 μM nCOV_N1 forward primer, 0.5 μM nCOV_N1 reverse primer, 0.125 μM nCOV_N1 probe, 0.3 μL of the GoScript Reverse Transcriptase Mix, and 1.0 μL of the target. The RT-qPCR protocol contains four stages: i) Stage 1 (2 min at 25 $^{\circ}\text{C}$), ii) Stage 2 (15 min at 50 $^{\circ}\text{C}$), iii) Stage 3 (2 min at 95 $^{\circ}\text{C}$), and iv) Stage 4 (40 cycles of 3 s at 95 $^{\circ}\text{C}$ and 30 s at 55 $^{\circ}\text{C}$). Real-time fluorescence quantitative detection was performed using the Bio-Rad CFX96 Touch Real-Time PCR Detection System.

3. Results and discussion

3.1. Overview of self-contained microfluidic system

Fig. 1A summarizes the workflow of SARS-CoV-2 detection in nasopharyngeal swab clinical samples using our self-contained microfluidic

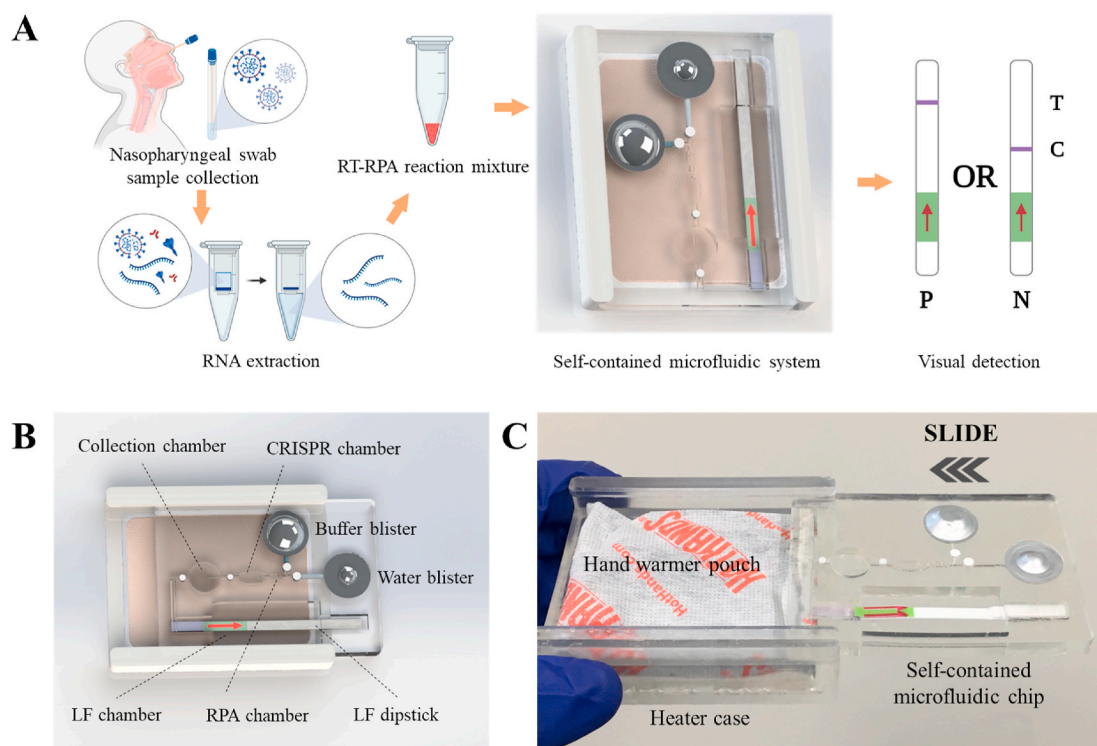


Fig. 1. Overview of SARS-CoV-2 detection in clinical samples using the self-contained microfluidic system. A) Workflow of SARS-CoV-2 detection with the self-contained microfluidic system. T, test band; C, control band. P and N represent positive result and negative result, respectively. B) Exploded view of the self-contained microfluidic system. The microfluidic chip mates with the hand warmer-powered heater case that provides chemical heat. LF, lateral flow. C) Photograph of the self-contained microfluidic system, including the self-contained microfluidic chip and hand warmer-powered heater case.

system. First, the viral RNA samples are extracted from swab samples collected from patients. Next, the master mix of the RT-RPA amplification reaction is prepared by adding the extracted RNA and introducing it into the microfluidic chip for instrument-free molecular detection. Ultimately, the visual detection results can be directly read by the naked eye against a lateral flow dipstick (Fig. 1A). The self-contained microfluidic system mainly consists of: i) one self-contained microfluidic chip and ii) one disposable, hand warmer-powered heater case (Fig. 1B and C). The microfluidic chip contains several functional units: i) the RT-RPA reaction chamber ($\sim 8 \mu\text{L}$), ii) the CRISPR reaction chamber ($\sim 30 \mu\text{L}$), iii) blisters for liquid storage, iv) the collection chamber ($\sim 300 \mu\text{L}$), and v) the lateral flow detection chamber ($\sim 2 \text{ mL}$). The dimensions of the reaction chambers (Fig. S1) are based on our optimized RT-RPA/CRISPR reaction protocol. The lateral flow detection chamber with a relatively large volume not only holds the lateral flow dipstick but also serves as a buffer container when the blisters are compressed in the closed, self-contained microfluidic chip. To facilitate point-of-care diagnostic application, the CRISPR-Cas12a reagents are lyophilized in the CRISPR reaction chamber, eliminating the need for cold chain. In addition, the water and dilution buffer, respectively, are pre-stored in the water blister and buffer blister. The chip integrates with a simple, portable, hand warmer-powered heater case and can easily slide in and out (Fig. 1B and C). The heater case uses a low-cost, disposable hand warmer pouch ($\sim \$0.3/\text{pouch}$) to provide chemical heat for on-chip RT-RPA amplification and CRISPR cleavage reaction, enabling electricity-free molecular detection. Overall, the self-contained microfluidic system is suitable for instrument-free detection of SARS-CoV-2 at the point of care.

3.2. Contamination-free visual detection of the self-contained microfluidic chip

The visual detection process of the self-contained microfluidic

system is schematically illustrated in Fig. 2. It includes four main steps: i) RT-RPA amplification, ii) CRISPR-Cas12a cleavage, iii) sample dilution, and iv) lateral flow detection. In the presence of the SARS-CoV-2 RNA target sequences, the ssDNA-BF probe is cleaved by the CRISPR-Cas12a enzyme specifically activated by the RPA amplicons (Fig. 2B) due to its trans-cleavage activity (Li et al., 2021), which results in release of the FAM and the biotin molecule from the ssDNA-BF probe. When the CRISPR-cleaved products mix with dilution buffer, they contact the sample pad of the lateral flow dipstick. The lateral flow dipstick contains one test band and one control band, which are immobilized with anti-rabbit antibody and streptavidin, respectively (Fig. 2C). For positive samples, the anti-FITC antibody (rabbit)-coated AuNPs (gold nanoparticles) bind with the anti-rabbit antibody of the test band and generate purple signal. On the contrary, for negative samples, the ssDNA-BF probe is not cut and forms a complex with the anti-FITC antibody (rabbit)-coated AuNPs that binds the control band site (Fig. 2C). It should be mentioned that the test band and control band are swapped in the CRISPR/Cas-based detection compared with conventional lateral flow detection (CRISPR/Cas-based detection strategies). Fig. 2D shows images of lateral flow dipsticks for visual detection of both positive and negative samples in a self-contained microfluidic chip. The weak purple signal in the test band of the negative sample may be caused by the hook effect due to the reporter (CRISPR/Cas-based detection strategies). Therefore, the self-contained microfluidic chip provides a simple, easy-to-use, contamination-free, visual molecular diagnostics, eliminating the need for time-consuming pipetting and reagent transferring.

3.3. Hand warmer-powered portable heater

Rapid and high-efficiency nucleic acid-based molecular detection typically requires heating the reaction solution at the optimum temperature of the enzymes (e.g., polymerase, CRISPR enzyme) using an

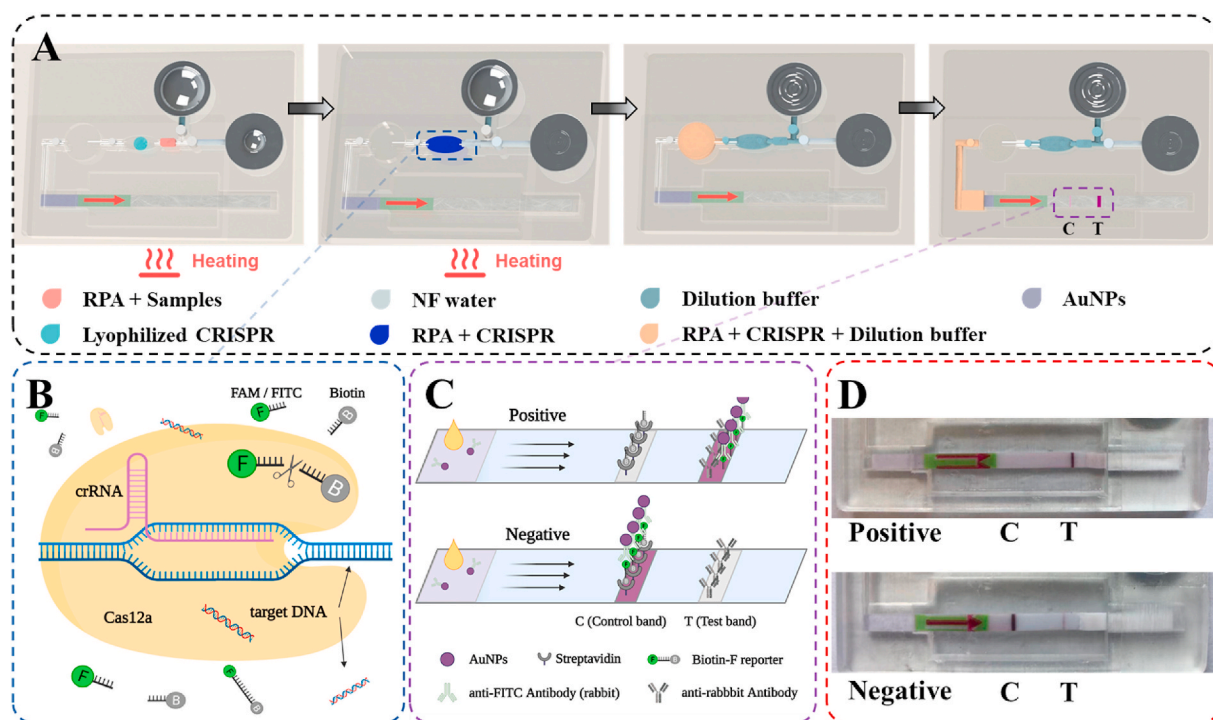


Fig. 2. Working principle of the self-contained microfluidic chip for contamination-free visual detection of SARS-CoV-2. A) Operating steps of the microfluidic system: RT-RPA amplification, CRISPR-Cas12a cleavage, dilution, and lateral flow detection. B) Activated CRISPR-Cas12a by RPA amplicons non-specifically cuts ssDNA-BF probe due to its trans-cleavage activity. C) Visual detection mechanism of the lateral flow dipstick. D) Photographs of lateral flow visual detection for positive and negative samples in the self-contained microfluidic chip.

electric heater (e.g., PCR machine, block heater). To eliminate the need for a complex electronic instrument and facilitate point-of-care diagnostics, we took advantage of an exothermic reaction to generate chemical heat for incubation of our self-contained microfluidic chip, enabling electricity-free molecular diagnostics. We used a commercially available hand warmer as the heating source because of its simplicity, low-cost, and wide heating temperature range. The hand warmer pouch contains chemicals for exothermic reaction, such as iron powder, salt, and activated carbon. The hand warmer can be activated by simply

removing its outer packaging and exposing it to oxygen in the air. To facilitate the operation, we employed one 3D-printed heater case (Fig. S1D) to hold the hand warmer pouch and integrated it with the microfluidic chip. In our RT-RPA/CRISPR assay, both RPA amplification and CRISPR detection are robust and can work at wide temperature ranges. Specifically, the optimal reaction temperature ranges of RPA amplification and the CRISPR cleavage reaction (e.g., EnGen® Lba Cas12a) are 37–42 °C and 25–48 °C, respectively, according to the vendors (EnGen Lba Cas12a (Cpf1) | NEB, RPA - The versatile

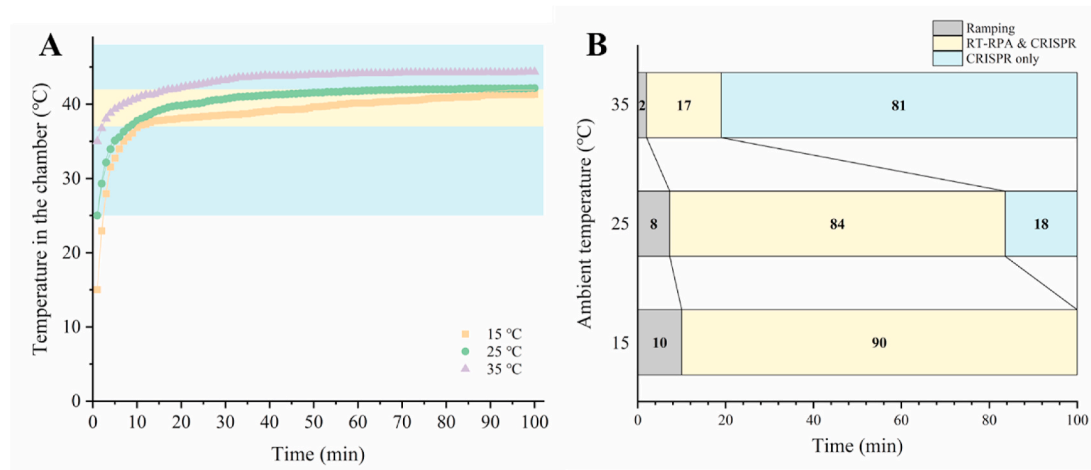


Fig. 3. Temperature measurement of the microfluidic chip in the portable heater powered by a hand warmer. A) The temperature of the reaction chamber in the self-contained microfluidic chip as a function of time at a variety of ambient temperatures (e.g., 15, 25, and 35 °C). The yellow zone represents the typical optimum reaction temperatures of 37–42 °C for the RPA amplification reaction. Both the yellow and blue zones represent the optimum reaction temperatures of 25–48 °C for the CRISPR-Cas12a (e.g., EnGen® Lba Cas12a) cleavage reaction. B) Different times for temperature ramping, RPA & CRISPR, and CRISPR cleavage reactions at different ambient temperatures (e.g., 15, 25, and 35 °C). (For interpretation of the references to color in this figure legend, the reader is referred to the Web version of this article.)

replacement to PCR). We first determined the effect of different ambient temperatures (e.g., 15, 25, 35 °C) on the reaction temperature of the chip (Fig. 3A). The higher the ambient temperature, the shorter the ramp time. When the ambient temperature increased from 15 to 35 °C, the time to maintain the temperature range of 37–42 °C for RPA amplification was shortened from 90 to 17 min (Fig. 3B). Importantly, this is adequate for the RPA amplification reaction, which typically completes within 10–15 min. In addition, we could maintain the chip temperature at a nearly uniform level (below 48 °C) for more than 90 min, which is longer than needed for the CRISPR cleavage reaction. Therefore, the hand warmer-powered heater provides a simple and affordable approach for electricity-free molecular diagnostics at the point of care.

3.4. Optimization of RT-RPA/CRISPR-based detection system

To optimize the design of our microfluidic chip, we first evaluated the effect of the volume ratio of the RT-RPA reaction product and CRISPR reaction solution on the lateral flow detection. We added different volumes of RT-RPA reaction product (e.g., 4, 8, 12, 16, and 19.5 μL) to the CRISPR reaction solution to obtain a final reaction volume of 30 μL . Interestingly, the color intensity of the test bands in the positive sample significantly increased with a decreasing RPA product volume (Fig. 4A), which may be attributed to a lower biocompatibility of the RPA reaction buffer with the downstream CRISPR cleavage reaction and lateral flow detection. However, when we used 4 μL RT-RPA product, we observed increased variance and background in the negative samples (Fig. 4A). Thus, we used 8 μL RT-RPA product in our experiments.

In addition, we further optimized the ssDNA-BF reporter concentration and dilution ratio of the CRISPR reaction product. We tested a series of concentrations of ssDNA-BF reporter ranging from 0.4 to 1.6 μM . The optimal reporter concentration ranged from 0.4 to 0.8 μM (Fig. 4B) and higher reporter concentrations resulted in decreasing intensity, which may be attributed to the hook effect (Rey et al., 2017; Sathishkumar and Toley, 2020). Considering the reagent cost, we selected 0.5 μM ssDNA-BF reporter for our experiments. To achieve highly sensitive lateral flow detection, it is necessary to dilute the CRISPR reaction products using dilution buffer. We determined the effect of the dilution ratio of CRISPR reaction solution and dilution buffer on the lateral flow test. With an increasing dilution ratio, the signal of the test band in the positive control increased and the background of the test band in the negative control decreased. Therefore, in our optimized

reaction system, we used 0.5 μM ssDNA-BF reporter and a 1:4 dilution ratio to develop our microfluidic chip.

3.5. Evaluation of the self-contained microfluidic system

Under the optimized experimental conditions, we evaluated the analytical sensitivity, specificity, and stability of the microfluidic system for SARS-CoV-2 detection. We determined the analytical sensitivity using a tenfold serial dilution of SARS-CoV-2 RNA samples and analyzed the experimental data using a one-way analysis of variance with Tukey's comparison test (Fozouni et al., 2021). With our microfluidic system, we can detect 100 copies of RNA per test (Fig. 5A and Fig. S2), which is comparable to that of conventional fluorescence-based RT-RPA/CRISPR detection (Fig. S3). With the increase of target RNA concentration, more Cas12a enzymes are activated by the RPA amplicons, which results in the increasing cleavage of the ssDNA-BF probe. Thus, the test band signal becomes strong and the control band signal becomes weak in the lateral flow dipstick (Fig. S2). To evaluate the specificity of the microfluidic system, we detected SARS-CoV-2 positive control, SARS-CoV positive control, and MERS-CoV positive control, and obtained excellent specificity (Fig. 5B and Fig. S4). To facilitate point-of-care testing, we lyophilized the CRISPR reagents in the CRISPR reaction chamber and evaluated the detection performance. For comparison, we included positive and negative control samples. The detection signals in the test bands were similar, indicating no obvious diminution of CRISPR enzyme cleavage activities (Fig. 5C and Fig. S5). The results indicate that our lyophilized reagents are stable during a relatively long storage period (e.g., more than 4 weeks). Thus, our self-contained microfluidic system offers a simple, easy-to-use, low-cost, and robust tool for SARS-CoV-2 detection that is suitable for point-of-care diagnostics in resource-limited settings.

3.6. Clinical validation of the self-contained microfluidic system for SARS-CoV-2 detection

To validate the clinical utility of our self-contained microfluidic system, we detected clinical nasopharyngeal swab samples, which includes 17 COVID-19 positive samples and 7 negative samples. We first confirmed the clinical samples by real-time RT-PCR (Fig. 6A). We also recorded the endpoint fluorescence images of the RT-PCR products (Fig. 6B and Fig. S6). All positive clinical samples, except for sample S7, showed strong color intensity on the test bands (Fig. 6C and Fig. S7), while the seven negative clinical samples did not. The false negative

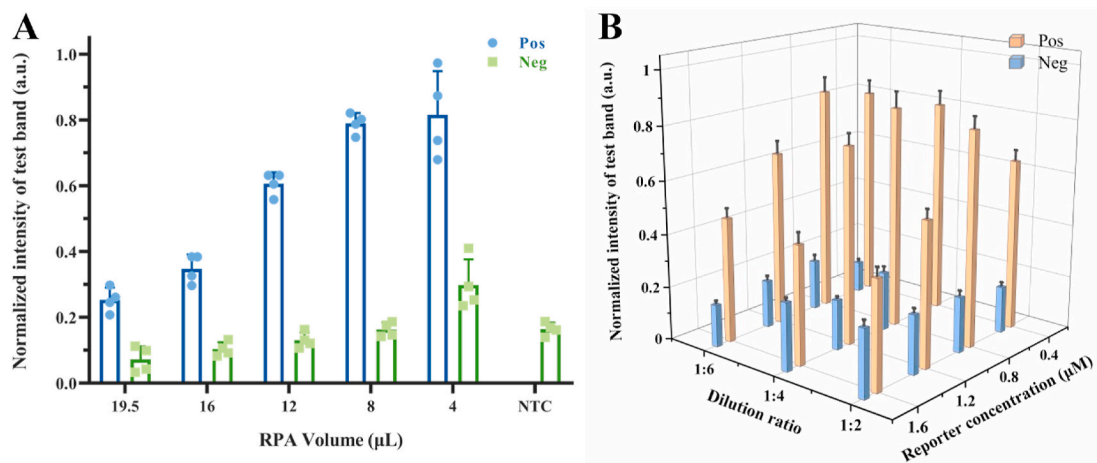


Fig. 4. Optimization of the RT-RPA/CRISPR reaction system. A) Optimization of the RT-RPA product volume in the CRISPR cleavage reaction system. Different volumes (e.g., 19.5, 16, 12, 8, and 4 μL) of RT-RPA reaction product were introduced into the CRISPR reaction solution with a final reaction volume of 30 μL . B) Optimization of ssDNA-BF reporter concentration and dilution ratio of CRISPR reaction solution and dilution buffer for the lateral flow detection. Pos is positive control with 10^5 copies of SARS-CoV-2 RNA target. Neg is negative control without target. All plots show mean \pm SD for $n \geq 4$ replicates.

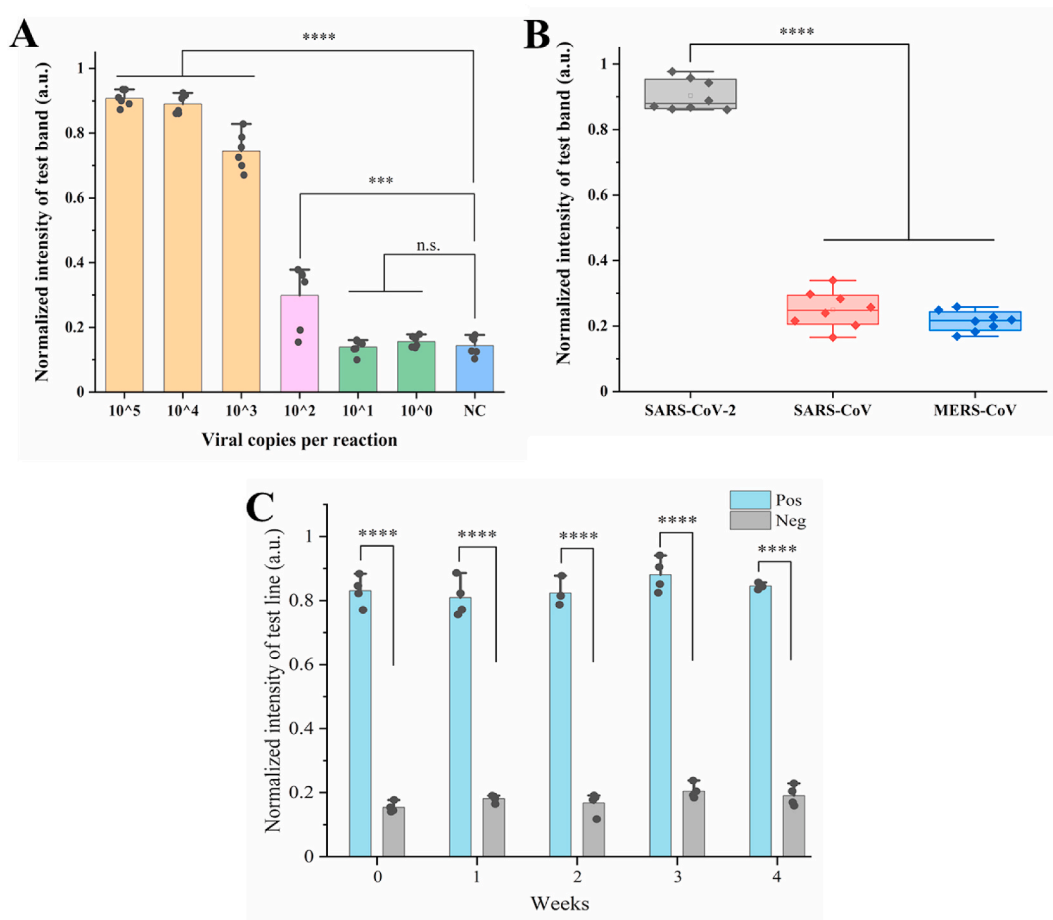


Fig. 5. Analytical performance evaluation of the self-contained microfluidic system. A) A tenfold serial dilution of SARS-CoV-2 RNA positive control ranging from 10^5 to 10^0 copies was detected by the microfluidic system. B) Specificity evaluation of the microfluidic system for SARS-CoV-2 detection. C) Stability evaluation of lyophilized CRISPR-Cas12a reaction reagents in the microfluidic chip. All statistical analyses were performed using a one-way analysis of variance with Tukey's comparison test, where n. s. = not significant with $p > 0.05$, and the asterisks (*, **, ***, ****) denote significant differences with p values (* = $0.001 < P \leq 0.05$, ** = $0.0001 < P \leq 0.001$, *** = $0.00001 < P \leq 0.0001$, **** = $P \leq 0.00001$). All plots show mean \pm SD for $n \geq 4$ replicates.

result of sample S7 is likely attributed to its low copy number as shown in Fig. 6A. According to a previous study (Vogels et al., 2021), a clinical sample with a quantification cycle (Cq) value of above 35 corresponds to ~ 10 copies of SARS-CoV-2 RNA. Thus, this result is consistent with a weak fluorescence signal in the endpoint fluorescence image of the RT-PCR product (Fig. 6B). It should be pointed out that our self-contained microfluidic system is more suitable to qualitative detection (Yes/No) due to the separate RT-RPA pre-amplification. Next, we analyzed the clinical performance of our microfluidic system by using a confusion matrix. With RT-qPCR as the gold standard, we achieved a sensitivity of 94.1%, specificity of 100%, and accuracy of 95.8% for SARS-CoV-2 detection (Fig. 6D). Thus, our self-contained microfluidic system demonstrates potential for simple, sensitive, instrument-free, clinical diagnostics of SARS-CoV-2 at the point of care.

4. Conclusion

In this study, we developed a simple, instrument-free, self-contained microfluidic system for SARS-CoV-2 detection at the point of care. The microfluidic system can detect 100 copies of SARS-CoV-2 RNA target. Further, we clinically validated the microfluidic system by testing clinical samples and showing excellent performance with a sensitivity of 94.1%, specificity of 100%, and accuracy of 95.8%. Our self-contained microfluidic system offers several advantages: i) Self-contained, on-chip reagent storage. By lyophilizing the CRISPR reagents into the reaction chamber and pre-storing the liquid solutions in the blisters, the

developed microfluidic system can be easily operated and transported without the need for cold chain, which is ideal for point-of-care testing by a minimally trained individual. ii) Instrument-free detection. By taking advantage of exothermic heat of the hand warmer, we developed a low-cost, disposable chemical heater for RPA amplification and the CRISPR cleavage reaction without the need for expensive electronic equipment. By combining this feature with lateral flow testing technology, we achieved instrument-free detection of SARS-CoV-2. iii) Contamination-free nucleic acid-based molecular diagnostics. Unlike previously reported CRISPR-based nucleic acid diagnostic assays, our self-contained microfluidic chip combines RT-RPA amplification, CRISPR reaction, and lateral flow visual detection in single, closed microfluidic platform, minimizing the contamination risk during amplicon transferring and simplifying the detection operation. In the future, we will further integrate the nucleic acid extraction module into the microfluidic chip to develop a fully integrated "sample-to-result" molecular diagnostic platform (Kadimisetty et al., 2018). If either a wider ambient temperature range or a more precise temperature control are needed, we will add phase change material into the heater case to regulate the temperature (Liao et al., 2016). Overall, our simple, instrument-free molecular diagnostic technology demonstrates great potential for rapid detection of COVID-19 and other infectious diseases at the point of care, especially in resource-limited settings, where there is a critical shortage of electricity access, funds, and well-trained healthcare professionals.

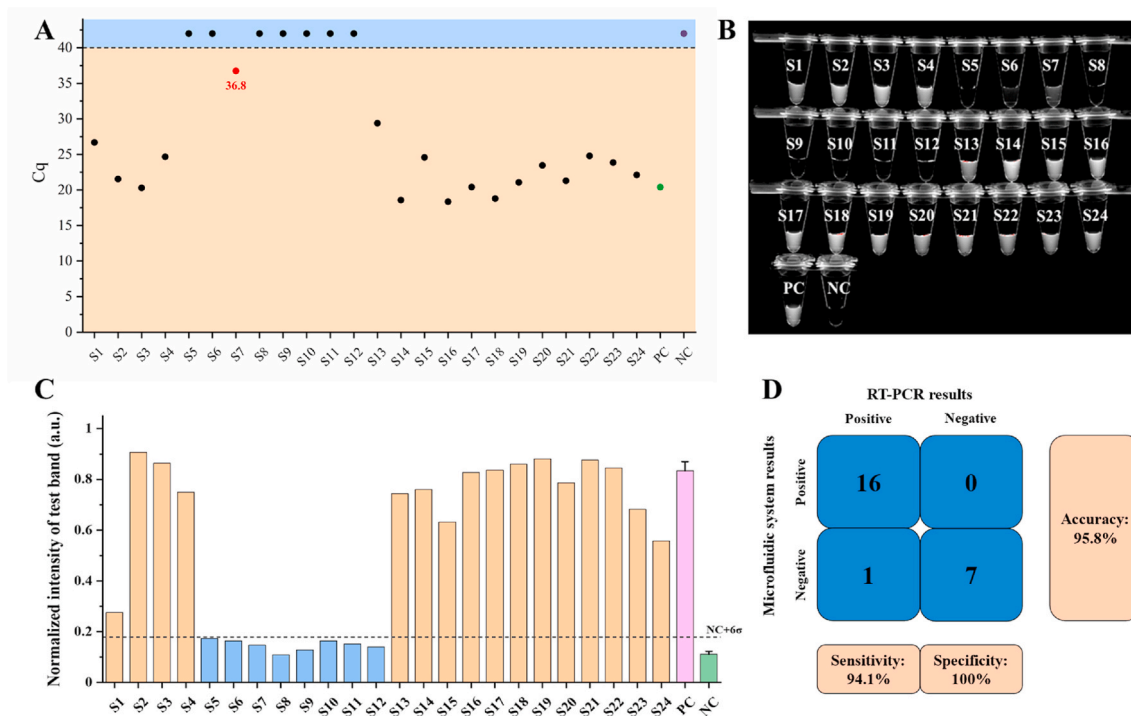


Fig. 6. SARS-CoV-2 detection in clinical swab samples by using the self-contained microfluidic system. A) Cq values of 24 clinical swab samples by RT-qPCR. B) Endpoint fluorescence image of RT-PCR products of 24 clinical samples under the ChemiDoc MP Imaging System. C) Normalized signal intensity of the test band on the lateral flow dipstick in the microfluidic chip for clinical sample detection. PC and NC are, respectively, positive control and negative control. D) Confusion matrix of the clinical performance of the microfluidic system. The RT-qPCR results are considered the standard. The sensitivity, specificity, and accuracy of the microfluidic system were 94.1%, 100%, and 95.8%, respectively.

CRedit authorship contribution statement

Ziyue Li: Conceptualization, Methodology, Validation, Investigation, Data curation, Formal analysis, Writing – original draft, Writing – review & editing. **Xiong Ding:** Investigation, Data curation, Formal analysis, Validation, Writing – review & editing. **Kun Yin:** Data curation, Formal analysis, Validation, Writing – review & editing. **Lori Avery:** Resources, Validation, Writing – review & editing. **Enrique Ballesteros:** Resources, Writing – review & editing. **Changchun Liu:** Conceptualization, Methodology, Investigation, Funding acquisition, Project administration, Supervision, Writing – original draft, Writing – review & editing.

Declaration of competing interest

The authors declare that they have no known competing financial interests or personal relationships that could have appeared to influence the work reported in this paper.

Acknowledgments

The work was supported, in part, by the National Institutes of Health, United States, R01 EB023607 and R61 AI154642.

Appendix A. Supplementary data

Supplementary data to this article can be found online at <https://doi.org/10.1016/j.bios.2021.113865>.

References

Ali, Z., Aman, R., Mahas, A., Rao, G.S., Tehseen, M., Marsic, T., Salunke, R., Subudhi, A. K., Hala, S.M., Hamdan, S.M., Pain, A., Alofi, F.S., Alsomali, A., Hashem, A.M.,

- Khogeer, A., Almontashiri, N.A.M., Abedalthagafi, M., Hassan, N., Mahfouz, M.M., 2020. *Virus Res.* 288, 198129.
- CDC, 2020. Real-Time RT-PCR Diagnostic Panel for Emergency Use Only, 3. Cdc Eua, pp. 1–42.
- EnGen Lba Cas12a (Cpf1) | NEB. URL: <https://www.neb.com/products/m0653-engen-lba-cas12a-cpf1#Product-Information>. (Accessed 22 October 2021).
- Fozouni, P., Son, S., Díaz de León Derby, M., Knott, G.J., Gray, C.N., D'Ambrosio, M.V., Zhao, C., Switz, N.A., Kumar, G.R., Stephens, S.I., Boehm, D., Tsou, C.L., Shu, J., Bhuiya, A., Armstrong, M., Harris, A.R., Chen, P.Y., Osterloh, J.M., Meyer-Franke, A., Joehnk, B., Walcott, K., Sil, A., Langelier, C., Pollard, K.S., Crawford, E. D., Puschnik, A.S., Phelps, M., Kistler, A., DeRisi, J.L., Doudna, J.A., Fletcher, D.A., Ott, M., 2021. *Cell* 184, 323–333 e9.
- Kadimisetty, K., Song, J., Doto, A.M., Hwang, Y., Peng, J., Mauk, M.G., Bushman, F.D., Gross, R., Jarvis, J.N., Liu, C., 2018. *Biosens. Bioelectron.* 109, 156–163.
- Lateral Flow Readout » CRISPR/Cas-based detection strategies. URL: <https://www.milena-biotech.com/en/tips-lateral-flow-readouts-crispr-cas-strategies/>. (Accessed 22 October 2021).
- Li, Z., Ding, X., Yin, K., Xu, Z., Cooper, K., Liu, C., 2021. *Biosens. Bioelectron.* 192, 113498.
- Liao, S.C., Peng, J., Mauk, M.G., Awasthi, S., Song, J., Friedman, H., Bau, H.H., Liu, C., 2016. *Sensors Actuators, B Chem.* 229, 232–238.
- Patchsung, M., Jantarug, K., Pattama, A., Aphicho, K., Suraritdechachai, S., Meesawat, P., Sappakhaw, K., Leelahakorn, N., Ruenkam, T., Wongsatit, T., Athipanyasilp, N., Eiamthong, B., Lakkanasirorat, B., Phoodokmai, T., Niljianskul, N., Pakotiprapha, D., Chanarat, S., Homchan, A., Tinikul, R., Kamutira, P., Phiwkaow, K., Soithongcharoen, S., Kantiwiriyawanitch, C., Pongsupasa, V., Trisrivirat, D., Jaroensuk, J., Wongnate, T., Maenpuen, S., Chaibyen, P., Kammerdnakta, S., Swangsri, J., Chuthapisith, S., Sirivatanauksorn, Y., Chaimayo, C., Sutthent, R., Kantakamalakul, W., Joung, J., Ladha, A., Jin, X., Gootenberg, J.S., Abudayyeh, O.O., Zhang, F., Horthongkham, N., Uttamapinant, C., 2020. *Nat. Biomed. Eng.* 4, 1140–1149.
- Ramachandran, A., Huyke, D.A., Sharma, E., Sahoo, M.K., Huang, C., Banaei, N., Pinsky, B.A., Santiago, J.G., 2020. *Proc. Natl. Acad. Sci. Unit. States Am.* 117, 29518–29525.
- Rey, E.G., O'Dell, D., Mehta, S., Erickson, D., 2017. *Anal. Chem.* 89, 5095–5100.
- RPA - The versatile replacement to PCR. URL: <https://www.twistdx.co.uk/en/rpa>. (Accessed 22 October 2021).
- Sathishkumar, N., Toley, B.J., 2020. *Sensors Actuators, B Chem.* 324, 128756.
- Tian, B., Minero, G.A.S., Fock, J., Dufva, M., Hansen, M.F., 2020. *Nucleic Acids Res.* 48, E30.
- Vogel, C.B.F., Brito, A.F., Wyllie, A.L., Fauver, J.R., Ott, I.M., Kalinich, C.C., Petrone, M. E., Casanovas-Massana, A., Catherine Muenker, M., Moore, A.J., Klein, J., Lu, P., Culligan, Lu, Jiang, A., Kim, X., Kudo, D.J., Mao, E., Moriyama, T., Oh, M., Park, J.E.,

- Silva, A., Song, J., Takahashi, E., Taura, T., Tokuyama, M., Venkataraman, M., Weizman, A., Wong, O.-E., Yang, P., Cheemarla, Y., White, N.R., Lapidus, E.B., Earnest, S., Geng, R., Vijayakumar, B., Odio, P., Fournier, C., Bermejo, J., Farhadian, S., Dela Cruz, S., Iwasaki, C.S., Ko, A., Landry, A.I., Foxman, M.L., Grubaugh, E.F., D, N., 2020. *Nat. Microbiol.* 510 (5), 1299–1305, 2020.
- Vogels, C.B.F., Watkins, A.E., Harden, C.A., Brackney, D.E., Shafer, J., Wang, J., Caraballo, C., Kalinich, C.C., Ott, I.M., Fauver, J.R., Kudo, E., Lu, P., Venkataraman, A., Tokuyama, M., Moore, A.J., Muenker, M.C., Casanovas-Massana, A., Fournier, J., Bermejo, S., Campbell, M., Datta, R., Nelson, A., Dela Cruz, C.S., Ko, A.I., Iwasaki, A., Krumholz, H.M., Matheus, J.D., Hui, P., Liu, C., Farhadian, S.F., Sikka, R., Wyllie, A.L., Grubaugh, N.D., Anastasio, K., Askenase, M. H., Batsu, M., Bickerton, S., Brower, K., Bucklin, M.L., Cahill, S., Cao, Y., Courchaine, E., DeLuliis, G., Earnest, R., Geng, B., Goldman-Israelow, B., Handoko, R., Khoury-Hanold, W., Kim, D., Knaggs, L., Kuang, M., Lapidus, S., Lim, J., Linehan, M., Lu-Culligan, A., Martin, A., Matos, I., McDonald, D., Minasyan, M., Nakahata, M., Naushad, N., Nouws, J., Obaid, A., Odio, C., Oh, J.E., Omer, S., Park, A., Park, H.-J., Peng, X., Petrone, M., Prophet, S., Rice, T., Rose, K.-A., Sewanan, L., Sharma, L., Shaw, A.C., Shepard, D., Smolgovsky, M., Sonnert, N., Strong, Y., Todeasa, C., Valdez, J., Velazquez, S., Vijayakumar, P., White, E.B., Yang, Y., 2021. *Med* 2, 263–280.e6.
- WHO Coronavirus (COVID-19) Dashboard. URL: <https://covid19.who.int/>. (Accessed 22 October 2021).
- Wang, R., Qian, C., Pang, Y., Li, M., Yang, Y., Ma, H., Zhao, M., Qian, F., Yu, H., Liu, Z., Ni, T., Zheng, Y., Wang, Y., 2021. *Biosens. Bioelectron.* 172, 112766.